

Visible light driven water splitting through an innovative Cu-treated- δ -MnO₂ nanostructure: probing enhanced activity and mechanistic insights

Kaushik Natarajan^a, Mohit Saraf^a and Shaikh M. Mobin^{*a,b,c}

^aDiscipline of Metallurgy Engineering and Materials Science, ^bDiscipline of Chemistry, ^cDiscipline of Biosciences and Biomedical Engineering, Indian Institute of Technology Indore, Simrol, Khandwa Road, Indore 453552, India

*Email: xray@iiti.ac.in

Tel: +91731 2438 762

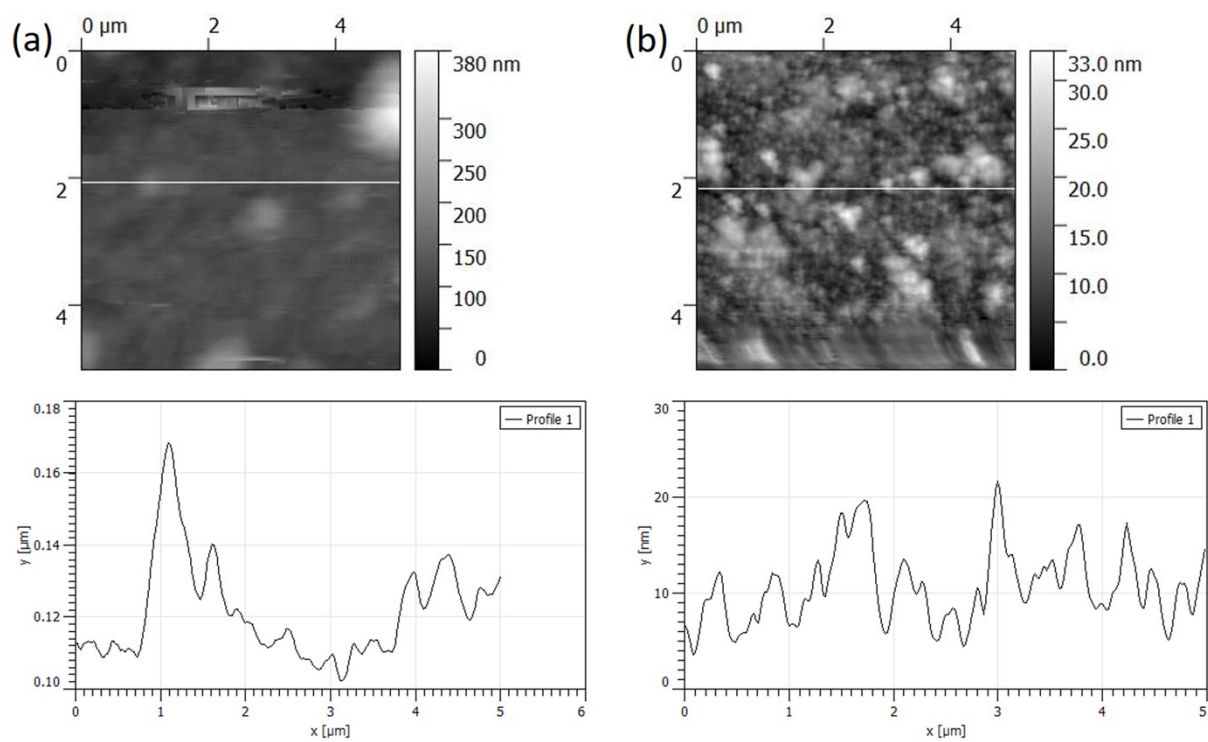


Fig. S1 AFM analysis of (a) δ -MnO₂ and (b) Cu- δ -MnO₂ thin film samples (over a 5 $\mu\text{m} \times 5 \mu\text{m}$ range).

The actual surface area and the surface roughness of some of the prepared samples have been estimated by AFM measurements as listed in **Table S1** below.

Table S1. AFM imaging results for the prepared samples

Sample	Image area (μm^2)	Root-mean square roughness, R_q (nm)	Average roughness, R_a (nm)	R_q/R_a	Surface area (μm^2)	Surface roughness parameter (R_s)
$\delta\text{-MnO}_2$	25	20.6610	35.4991	0.582	25.26	1.0104
$\text{Cu-}\delta\text{-MnO}_2$	25	35.304	45.4798	0.7762	26.72	1.0688

Data presented above indicates an increased surface area for the $\text{Cu-}\delta\text{-MnO}_2$ samples.

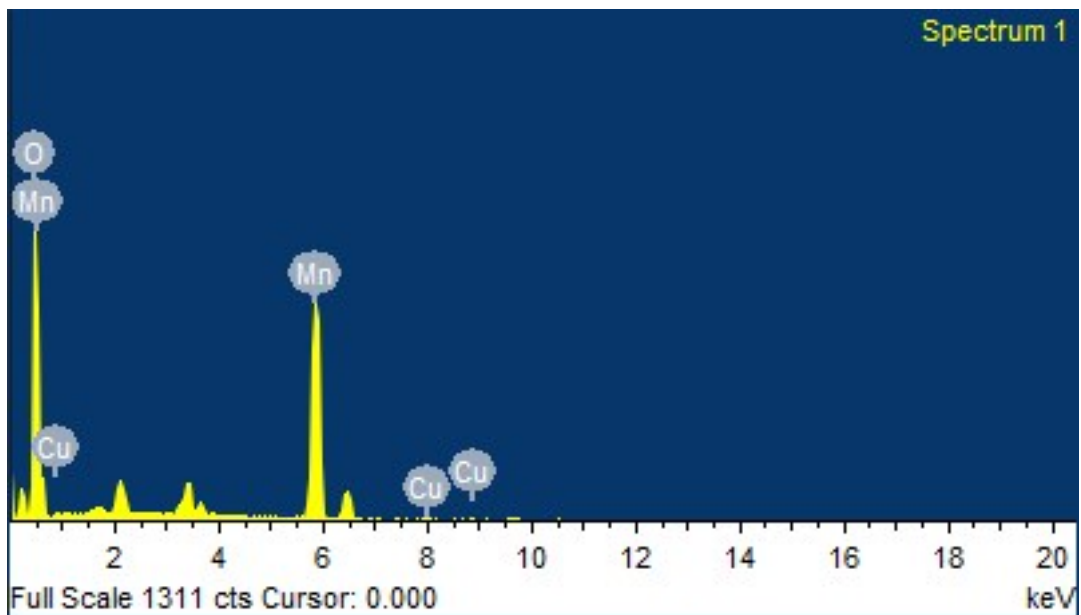


Fig. S2 EDX analysis of the prepared Cu- δ -MnO₂ thin film.

Processing option: All elements analyzed (Normalized)
 Number of iterations = 2

Standard:

O SiO₂ 1-Jun-1999 12:00 AM
 Mn Mn 1-Jun-1999 12:00 AM
 Cu Cu 1-Jun-1999 12:00 AM

Element	Weight%	Atomic%
O K	38.30	68.14
Mn K	60.25	31.21
Cu K	1.46	0.65
Totals	100.00	

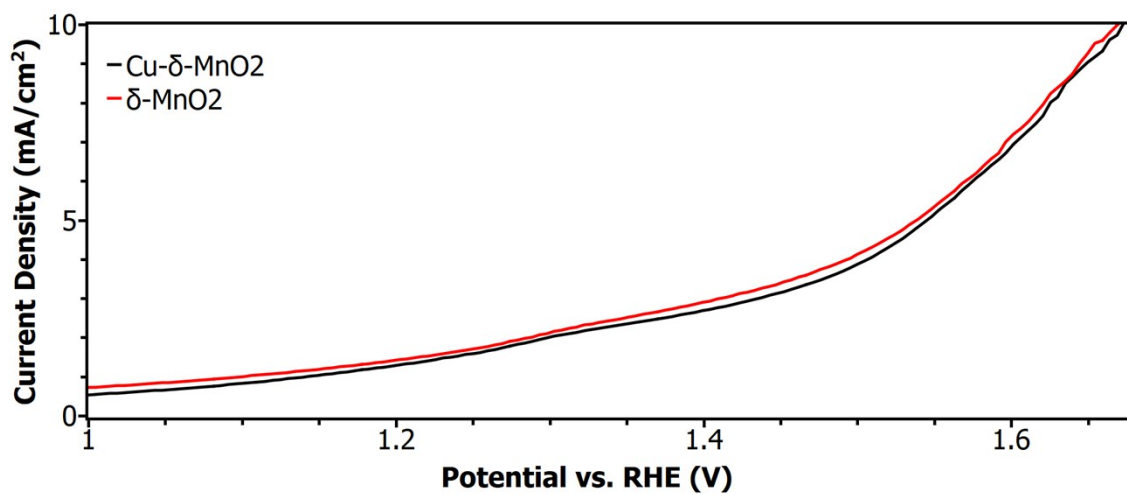


Fig. S3 Current density-voltage curve of the as-prepared thin film samples for anodic scan (water oxidation) in 1 M NaOH solution (pH = ~13), using Ag/AgCl reference electrode and Pt counter electrode.

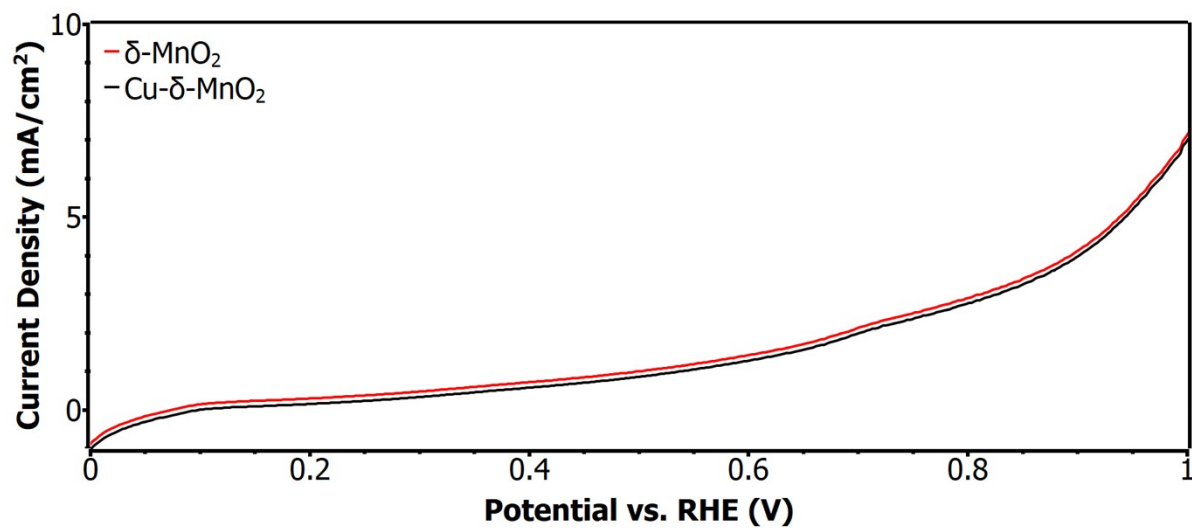


Fig. S4 Current density-voltage curve of the as-prepared thin film samples for cathodic scan under dark conditions in 1 M Na₂SO₄ solution (pH = 4.0), using Ag/AgCl reference electrode and Pt counter electrode.

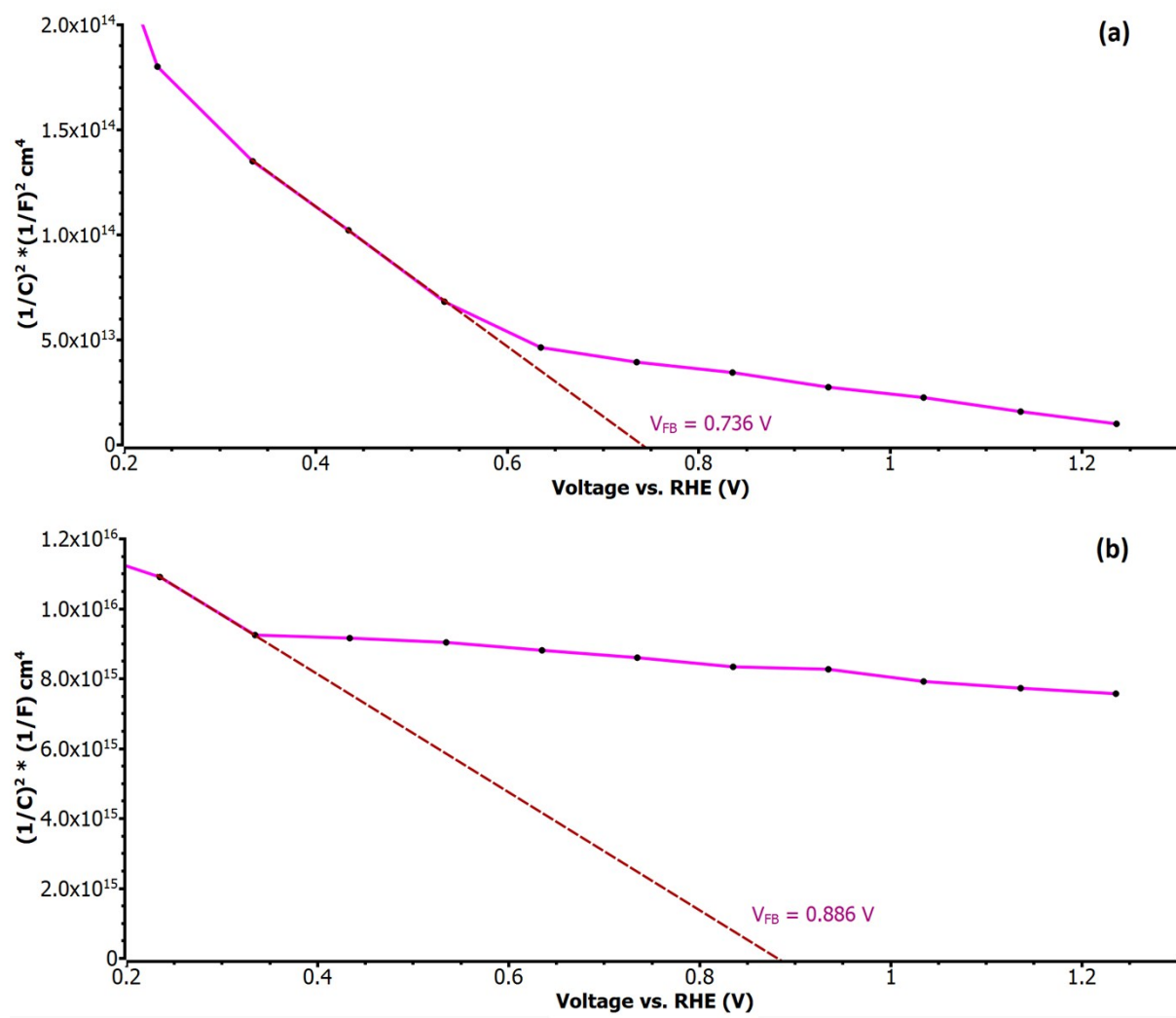


Fig. S5 Mott-Schottky plots of Cu- δ -MnO₂ film (a) in dark and (b) in illumination. Note: Mott-Schottky of δ -MnO₂ film is the same as (a).

Table S2. Comparison table for anodic electrocatalytic current: overpotential required to reach 10 mA/cm² anodic current for water oxidation

Material	Electrolyte	Overpotential (vs. RHE) to reach 10 mA/cm²	Reference
Cu ₂ S in graphitic carbon nanofibers	0.25 M phosphate buffer	401 mV	[i]
CoNi double hydroxide/CoO	1 M KOH	300 mV	[ii]
CoNi layered double hydroxide	0.1 M Phosphate buffer	390 mV	[iii]
CuO	0.1 M KBi	430 mV	[iv]
Cu(OH) ₂	0.1 M KBi	550 mV	[v]
MnO _x	0.2 M Borate Buffer	~520 mV	[vi]
δ-MnO ₂	1 M NaOH	440 mV	This work

XPS Acquisition Parameters

A. Survey Scan

Acquisition Parameters :	
Parameter	
Total acquisition time	54.4 secs
Number of Scans	2
Source Gun Type	Al K Alpha
Spot Size	900 μm
Lens Mode	Standard
Analyser Mode	CAE : Pass Energy 150.0 eV
Energy Step Size	1.000 eV
Number of Energy Steps	1361

B. C1s scan

Acquisition Parameters :	
Parameter	
Total acquisition time	1 mins 35.2 secs
Number of Scans	5
Source Gun Type	Al K Alpha
Spot Size	900 μm
Lens Mode	Standard
Analyser Mode	CAE : Pass Energy 20.0 eV
Energy Step Size	0.050 eV
Number of Energy Steps	381

C. O1s scan

Acquisition Parameters :	
Parameter	
Total acquisition time	1 mins 40.2 secs
Number of Scans	5
Source Gun Type	Al K Alpha
Spot Size	900 μm
Lens Mode	Standard
Analyser Mode	CAE : Pass Energy 20.0 eV
Energy Step Size	0.050 eV
Number of Energy Steps	401

D. Mn2p scan

Acquisition Parameters :	
Parameter	
Total acquisition time	2 mins 20.2 secs
Number of Scans	5
Source Gun Type	Al K Alpha
Spot Size	900 μm
Lens Mode	Standard
Analyser Mode	CAE : Pass Energy 20.0 eV
Energy Step Size	0.050 eV
Number of Energy Steps	561

E. Mn3p scan

Acquisition Parameters :	
Parameter	
Total acquisition time	1 mins 15.2 secs
Number of Scans	5
Source Gun Type	Al K Alpha
Spot Size	900 μm
Lens Mode	Standard
Analyser Mode	CAE : Pass Energy 20.0 eV
Energy Step Size	0.050 eV
Number of Energy Steps	301

F. Mn3s scan

Acquisition Parameters :	
Parameter	
Total acquisition time	2 mins 0.2 secs
Number of Scans	5
Source Gun Type	Al K Alpha
Spot Size	900 μm
Lens Mode	Standard
Analyser Mode	CAE : Pass Energy 20.0 eV
Energy Step Size	0.050 eV
Number of Energy Steps	481

G. Cu2p scan

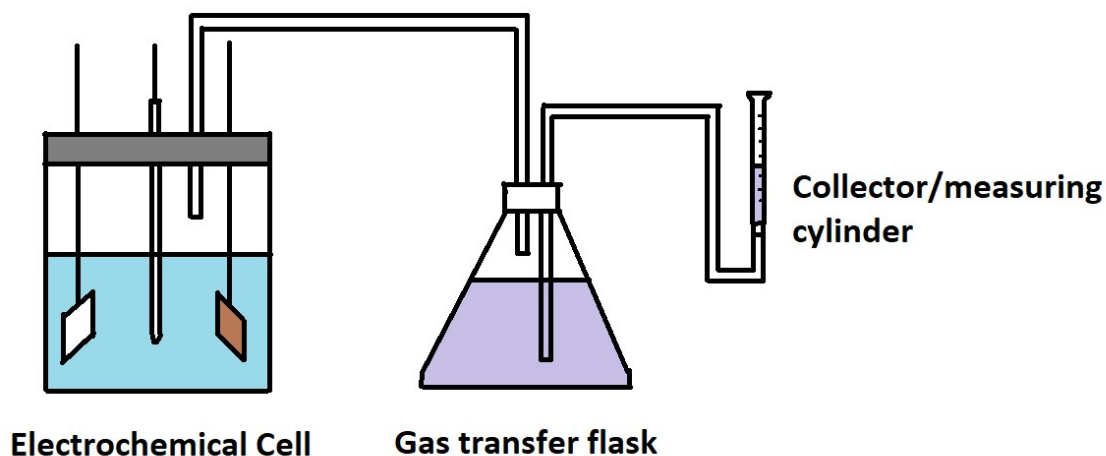
Acquisition Parameters :	
Parameter	
Total acquisition time	16 mins 40.8 secs
Number of Scans	25
Source Gun Type	Al K Alpha
Spot Size	900 μm
Lens Mode	Standard
Analyser Mode	CAE : Pass Energy 20.0 eV
Energy Step Size	0.050 eV
Number of Energy Steps	801

Calculation of Faradaic efficiency

Faradaic efficiency test was done using a closed apparatus as shown in **Scheme S1**. The apparatus consists of three sealed chambers: (1) A glass chamber comprising of three electrode cell in which gas production occurs; (2) A gas transfer compartment and (3) a water displacement cell consisting of a marked cylinder with 100 $\mu\text{L}/0.1$ ml increments.

The solutions in the reaction cell as well as the gas transfer compartment were first saturated with oxygen and hydrogen gases. Next, the reaction was started using the $\text{Cu-}\delta\text{-MnO}_2$ as working electrode and gas generation was started (either with positive voltage to working electrode in the case of oxygen evolution, or negative voltage with illumination from 1000 W/m^2 calibrated light source). This causes water level in graduated cylinder to rise. In this way all connecting tubes between compartments are now saturated with oxygen and hydrogen.

Finally, an electric charge of 3.0 Coulombs was passed through the working electrode until the water level in the graduated cylinder increased by 500 $\mu\text{L}/0.5$ ml. This change is associated with 2/3 hydrogen gas and 1/3 oxygen gas. After correcting for contributions from vapour pressure of water in the container(s), the proportion of hydrogen and oxygen obtained was determined in separate experiments and was found to be 321 μL and 161 μL respectively. Using gas laws, the quantity of gas produced was found to be 14.33 and 7.188 μmol respectively, which requires 2.766 and 2.775 coulombs respectively to generate. This corresponds to a Faradaic efficiency of 92.2% and 92.5%, for the hydrogen generation and oxygen evolution reactions respectively.



Scheme S1. Schematic of experimental setup used to measure gas generation by water displacement method.

Calculation for Faradaic efficiency of Hydrogen and Oxygen Evolution Processes

In an ideal system with 100% Faradaic efficiency and no side reactions; 1 coulomb of current into an electrochemical cell generates 5.18 μmol of H_2 and 2.59 μmol of O_2 . This is based on the following equation:

$$\text{No. of moles} = \text{Coulombs} / (\text{Unsigned Numeric Charge on the ion} \times \text{Faraday Constant})$$

Thus, for 3 coulombs of charge given to the electrochemical cell, the quantities of H₂ and O₂ would be 15.54 μmol and 7.77 μmol, respectively.

Given the experimental conditions essentially correspond to room temperature and atmospheric pressure and that the ideal gas laws hold adequately in such conditions, we can then use gas laws *i.e.* 1 mol = 22.4 L, and so 1 μmol = 22.4 μL to determine the exact quantities of H₂ and O₂ evolved in the experiments.

In the experimental setup, 3 coulombs of electric charge was passed through to the electrochemical cell till a 500 μL displacement was observed. Of this, the component corresponding to the vapour phase H₂O was subtracted using the vapour pressure tables wherein P_{H₂O} (partial pressure of water) at 28 °C is 28.4 torr. At the time of the initial setup, since the entire apparatus is air saturated with water-based electrolyte, the total pressure in the container(s) is 760 torr + 28.4 torr = 788.4 torr. After the experiment has completed and appropriate displacement obtained, the component corresponding to the vapour pressure of water is subtracted from the total pressure (= 788.4 torr) and thus the value of displacement caused due to O₂ and H₂ gases without the involvement of water vapour is found to be $(760/788.4) * (500 \mu\text{L})$, which gives us a value of 482 μL approximately. With 3 coulombs of energy passing; this 482 μl is attributed to a 2/3rd contribution of H₂ gas and 1/3rd contribution of O₂ gas, the proportions of the displacement thus obtained work out to be 321 μL and 161 μL for the displacements caused by H₂ gas and O₂ gas respectively.

Based on this method, the obtained quantities in μmol for the H₂ and O₂ gases produced in separate experiments are determined to be $321/22.4 = 14.33 \mu\text{mol}$ and $161/22.4 = 7.188 \mu\text{mol}^*$

* = *Original value is 7.1875 μmol, which is rounded off to 7.188 μmol.*

When compared to the optimal (100% efficient) quantities of 15.54 and 7.77 μmol respectively for 3 coulombs of input charge; we find the faradaic efficiency to be 92.2% and 92.5% for the Hydrogen Generation and Oxygen Evolution Reactions, respectively.

If the contribution from water vapour in the container(s) is ignored; the entire 500 μL is considered as being caused by the H₂/O₂ gas generation. In such a case, the quantities for H₂ and O₂ gases thus generated turn out to be 14.866 μmol and 7.466 μmol respectively, which correspond to Faradaic efficiencies of 95.66% and 96.09% respectively for the hydrogen generation and oxygen evolution reactions respectively.

Stability Testing

Photocurrent stability was tested at 0.2 V vs. RHE by using chronoamperometry to observe the decay of photocurrent over time in a standard three-electrode electrochemical cell comprising of 1 M Na₂SO₄ with pH adjusted to 4.0 as the electrolyte, Ag/AgCl reference electrode, Pt counter electrode and Cu- δ -MnO₂ as the working electrode with 1000 W/m² light source as described in main manuscript and 25 °C ambient temperature. It is observed that approximately 74.6% of initial photocurrent is retained after 7200 seconds of testing. The results may be seen below.

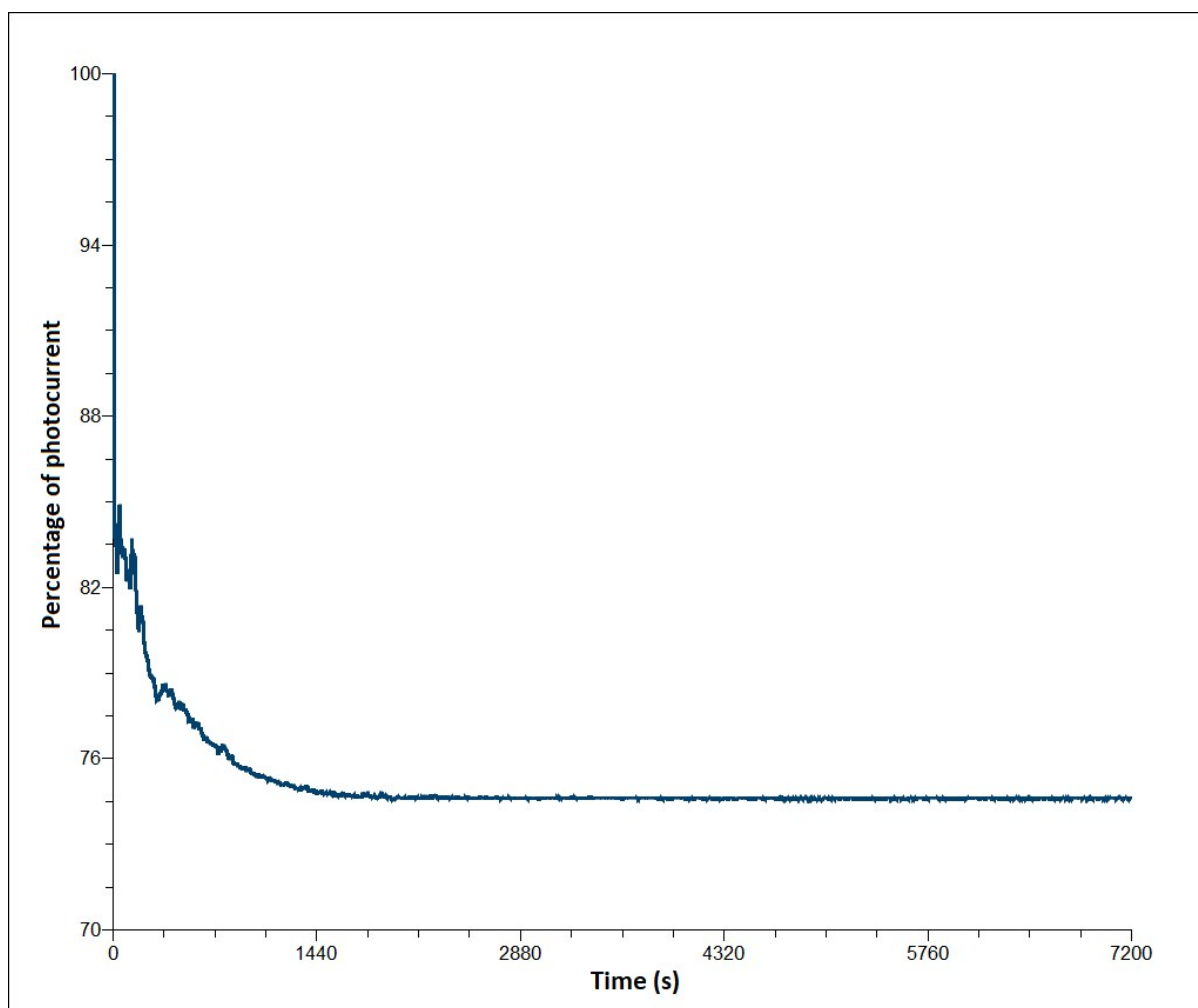


Fig. S6 Chronoamperometric curve expressed as percentage of initial photocurrent over time for Cu- δ -MnO₂ thin film on FTO glass substrate.

Electrochemical test to calculate recombination lifetimes

The EIS analysis was performed similarly to the other electrochemical tests; namely a three electrode configuration cell was used with Cu- δ -MnO₂ film on FTO glass substrate as the working electrode, a Pt counter electrode and Ag/AgCl reference electrode was utilised with input frequency range between 1 Hz and 10 MHz. The modelling was done based on a three RC series element circuit first described by Kumar et al. and is shown in Fig. S7, modelled against the electrochemical data described in the main manuscript. The results of the fitting are shown in Table S3 below. The values of τ_2 indicate effective recombination lifetime, while those of $\tau_1 (=R_1C_1)$ and $\tau_3 (=R_3C_3)$ are indicative of surface recombination lifetimes due to the presence of thin layers of oxide films at the film-to-substrate interface as well as the film-to-electrolyte interface^{viii}. The element R_s indicates the circuit series resistance.

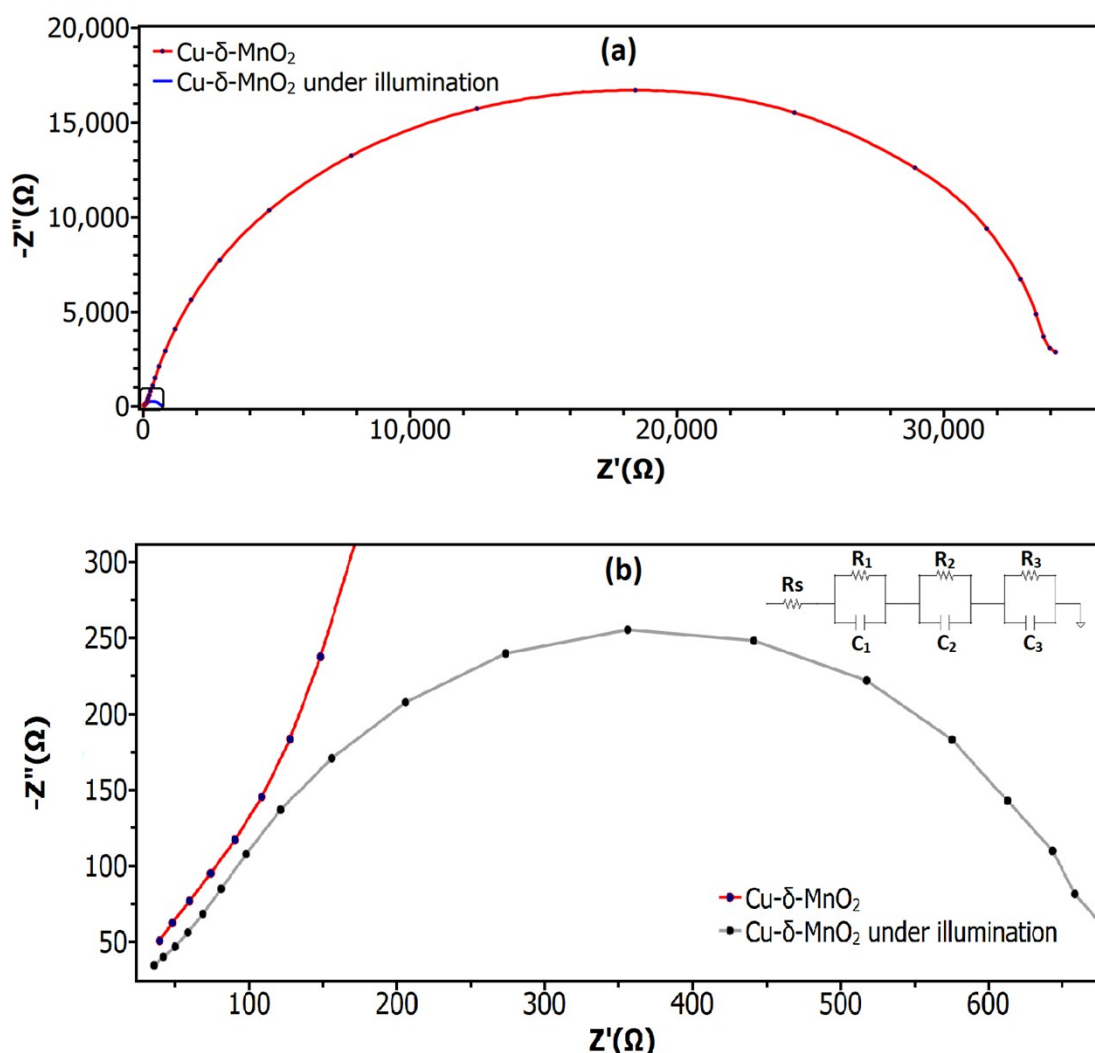


Fig. S7 (a) Electrochemical Impedance Spectrum of Cu- δ -MnO₂ films with and without illumination. (b) Zoomed portion of EIS spectrum of highlighted region. Inset shows equivalent circuit utilised for fitting the EIS spectra for calculation of recombination lifetime.

Table S3. Comparison of electrochemical parameters obtained by fitting EIS data against the circuit model described in inset of **Fig. S7**.

Parameter	R_s (Ω)	R₁ (Ω)	C₁ (F)	R₂ (Ω)	C₂ (F)	R₃ (Ω)	C₃ (Ω)	τ_1 (μs)	τ_2 (μs)	τ_3 (μs)
Cu- δ -MnO ₂ (dark)	28	553	2.915 $\times 10^{-7}$	110.6	4.814 $\times 10^{-8}$	3337.35	1.925 $\times 10^{-7}$	161.2	5.32	642.6
Cu- δ -MnO ₂ (illuminated)	20	195	1.348 $\times 10^{-6}$	48.72	3.363 $\times 10^{-7}$	425.40	2.733 $\times 10^{-6}$	263.6	16.39	1162

Conversion from Ag/AgCl scale to RHE scale

For all electrochemical measurements, the Nernst equation was used to draw equivalent scale from Ag/AgCl to RHE:

$$E_{RHE} = E_{Ag/AgCl} + 0.059 pH + E_{Ag/AgCl}^{\circ}$$

References:

- i. X. Zhao, L. Liu, Y. Zhang, H. Zhang and Y. Wang, *Nanotechnology*, 2017, **28**, 345402 (1-11).
- ii. J. Wu, Z. Ren, S. Du, L. Kong, B. Liu, W. Xi, J. Zhu and H. Fu, *Nano Res.*, 2016, **9**, 713-725.
- iii. R. Valdez, D. B. Grotjahn, D. K. Smith, J. M. Quintana and A. Olivas, *Int. J. Electrochem. Sci.*, 2015, **10**, 909-918.
- iv. X. Liu, S. Cui, Z. Sun, P. Du, *Electrochim. Acta*, 2015, **160**, 202-208.
- v. S. Cui, X. Liu, Z. Sun, and P. Du, *ACS Sustainable Chem. Eng.*, 2016, **4**, 2593-2600.
- vi. F. Zhou, F.; C. McDonnell-Worth, H. Li, J. Li, L. Spiccia and D. R. MacFarlane, *J. Mater. Chem. A*, 2015, **3**, 16642-16652.
- vii. S. Kumar, P. K. Singh, G. S. Chilana and S. R. Dhariwal, *Semicond. Sci. Technol.*, 2009, **24**, 095001 (1-8).